Environmental Research Papers
No. 35

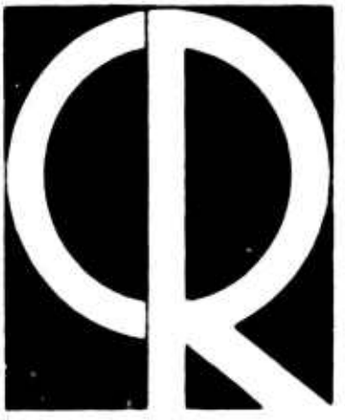

Geodetic Positioning From Simultaneous Optical Observations of the ANNA I-B Satellite

LYNDON L. SHELDON, Capt, USAF

DONALD H. ECKHARDT

TERRESTRIAL SCIENCES LABORATORY PROJECT 7600

AIR FORCE CAMBRIDGE RESEARCH LABORATORIES, OFFICE OF AEROSPACE RESEARCH, UNITED STATES AIR FORCE, L.G. HANSCOM FIELD, MASS

AFCRL-64-562
JULY 1964

Environmental Research Papers
No. 35

Geodetic Positioning From Simultaneous Optical Observations of the ANNA I-B Satellite

LYNDON L. SHELDON, Capt, USAF

DONALD H. ECKHARDT

TERRESTRIAL SCIENCES LABORATORY PROJECT 7600

AIR FORCE CAMBRIDGE RESEARCH LABORATORIES, OFFICE OF AEROSPACE RESEARCH, UNITED STATES AIR FORCE, L.G. HANSCOM FIELD, MASS

Abstract

Simultaneous photographic observations of flashes from the ANNA I-B geodetic satellite were made by Air Force PC-1000 cameras during the period September 1963 to January 1964. Geodetic position determinations using these ANNA observations indicate that the PC-1000 camera system used with the intervisible technique is capable of extending geodetic control to a proportional accuracy of better than 1/100,000.

Contents

Tables

Illustrations

Geodetic Positioning From Simultaneous Optical Observations of the ANNA 1-B Satellite

I. INTRODUCTION

The ANNA 1-B geodetic satellite was launched on 31 October 1962. Since that time many optical observations have been made utilizing the satellite in the orbital mode, the short arc mode, and with the intervisible technique.

This paper, the second in a series on geodetic determinations from ANNA optical observations, covers the intervisible technique during the period September 1963 to January 1964. Previously, ANNA short arcs were investigated under an AFCRL contract.[1] Azimuth determinations from simultaneous ANNA photographic observations have been completed recently.[2] Orbital techniques for geodesy using ANNA data are being evaluated at this time.

In this project, commonly known as the "Gulf Test," the simultaneous observation network was made up of ten PC-1000 cameras located in the southern United States (Table 1). The camera site layout, chosen for an Air Photographic and Charting Service rocket flare triangulation test, was used as a matter of expediency, although the station geometry was not the best.

In the Gulf Test, as in the whole ANNA project, the Air Force has utilized the optical portion of the ANNA geodetic satellite program through the participation of three agencies: Air Force Cambridge Research Laboratories (AFCRL), Air Photographic and Charting Service (APCS), and the Aeronautical Chart and Information Center (ACIC). AFCRL computed the look-angle information, scheduled the flash

(Received for publication 11 June 1964)

sequences, triggered the flashes with the emergency override system when necessary, and performed the final geodetic reductions. APCS distributed the look-angles and operated and maintained the PC-1000 stellar cameras. ACIC performed the plate reductions, forwarding right ascensions and declinations of the flash positions to AFCRL for use in the geodetic reductions.

The purpose of the Gulf Test is to prove-out a stereo-triangulation system that encompasses a satellite-borne light source, PC-1000 camera systems, a plate reduction method developed specifically for long focal length cameras,[3] and a computer program for intervisible geodetic reductions.[4]

2. SATELLITE BEACON

Although the ANNA satellite carries SECOR, an electronic ranging system, and the Transit doppler equipment in addition to the flashing light system, only the latter has direct application to this paper.

The ANNA optical beacon, developed for AFCRL by Edgerton, Germeshausen and Grier, Inc., consists of two pairs of xenon-filled stroboscopic lamps mounted in reflectors, one pair on the north face of the solar cell panel and one pair on the south face. Since the satellite is magnetically stabilized, one pair of lights is utilized when the satellite is north of the magnetic equator. A flash sequence is composed of five flashes spaced 5.6 sec apart. The energy per flash is 1100 joules. The flash duration is 1.2 msec, producing a light output of about 8800 candle-sec per flash. Under normal operation, flash times are inserted into the satellite memory from an injection station located at the Applied Physics Laboratory in Maryland when the satellite passes within range of the station. The timing of the flash sequences is controlled by the memory clock. At the predetermined times the clock initiates the flash sequences, to an accuracy of 0.1 to 0.5 msec.

An alternative method of initiating flash sequences, in the event of satellite memory problems, is afforded by the emergency override system (EMOS), which was located at AFCRL, Bedford, Mass., during the Gulf Test exercise. The EMOS (Figure 1), made up of an antenna, transmitter, and timing system, enables an operator to initiate flash sequences on command, to 1-msec accuracy. Absence of doppler tracking data, necessary for accuracy checks on the ANNA clock timing, has necessitated using the EMOS for executing flash sequences since 11 October 1963.

3. PC-1000 CAMERA SYSTEM

The PC-1000 (Figure 2), a fixed stellar camera, has a 1000-mm focal length, a 200-mm aperture, and a 10° square field of view. Type 103F emulsion photographic

Figure 1. Emergency Override System

plates were used to photograph the ANNA flashes simultaneously against star backgrounds that included stellar magnitudes as low as the 9th.

Figure 2. PC-1000 Geodetic Stellar Camera

A normal observation is made as follows. Two precalibration sequences of shutter openings separated by approximately 40 sec are taken with openings of 2, 1, 0.5, 0.3 and 0.1 sec, the shutter being closed for 15 sec between openings. Each recorded star gives rise to a trace of pointlike images. Fifteen seconds after the precalibration, the shutter is opened for 1 min to photograph the ANNA five-flash sequence, which produces flash images ranging from 40 to 70 microns in diameter, depending on the camera-satellite range. After the shutter is closed for a 15-sec period, a series of double postcalibrations is taken.

The final plate consists of a series of five-flash images recorded on a background of hundreds of control points provided by the star images. The control points selected are those that closely match the photographic characteristics of the flash images. This eliminates the measuring bias problem since the bias is the same for both the flash images and the measured control. An ANNA plate reduction

usually involves 60 to 70 stellar images corresponding to the double precalibration and postcalibration exposure times.

The flash directions from each observing station are determined from the plate measurements of control points and flash images. These are forwarded by ACIC to AFCRL in the form of topocentric right ascensions and declinations. Included with the flash directions are their standard deviations, which are by-products of the plate reduction program. These, together with the observing station positions and their assumed uncertainties, comprise the input for the intervisible (simultaneous observation) geodetic reduction program.

4. INTERVISIBLE ADJUSTMENT THEORY

The usual departure point for the adjustment of overdetermined systems, such as those stemming from the Gulf Test, is the method of least squares. This method is based rigorously on the method of maximum likelihood for normal deviates, which is the foundation on which the reduction technique for the Gulf Test systems is directly constructed.

The principle of the method of maximum likelihood is to maximize the likelihood function or its logarithm L with respect to the parameters to be adjusted θ^p, $p = 1, 2, \ldots, P$. Consider these parameters as the elements of a P-vector $\boldsymbol{\Theta}$. Then the conditions for a stationary point at $\boldsymbol{\Theta} = \hat{\boldsymbol{\Theta}}$ can be written

$$\left(\frac{\partial L}{\partial \theta^p}\right)_{\hat{\boldsymbol{\Theta}}} = 0, \qquad p = 1, 2, \ldots, P.$$

Suppose that $\tilde{\boldsymbol{\Theta}}$ is an approximation to $\boldsymbol{\Theta}$. By Taylor series expansion to the first order in $(\hat{\theta}^p - \tilde{\theta}^p)$, these conditions become

$$\left(\frac{\partial L}{\partial \theta^p}\right)_{\tilde{\theta}} + \sum_{q=1}^{P} \left(\frac{\partial^2 L}{\partial \theta^p \partial \theta^q}\right)_{\tilde{\boldsymbol{\Theta}}} (\hat{\theta}^q - \tilde{\theta}^q) = 0 \qquad p = 1, 2, \ldots, P.$$

Let the inverse of the matrix $-\left(\frac{\partial^2 L}{\partial \theta^p \partial \theta^q}\right)_{\tilde{\boldsymbol{\Theta}}}$ be $\left[\eta^{pq}\right]$. The first-order solution for $\hat{\boldsymbol{\Theta}}$ becomes

$$\hat{\theta}^p = \tilde{\theta}^p + \sum_{q=1}^{P} \eta^{pq} \left(\frac{\partial L}{\partial \theta^q}\right)_{\tilde{\boldsymbol{\Theta}}} \qquad p = 1, 2, \ldots, P. \tag{1}$$

This array is the form used in the iterative solutions of the Gulf Test networks. It can be shown that with such an iterative technique, $\hat{\Theta}$ converges in probability to the true parameter Θ and η^{pq} converges in probability to the expected value of $(\hat{\theta}^p - \theta^p)(\hat{\theta}^q - \theta^q)$, that is, $\left[\eta^{pq}\right]$ is the solution covariance matrix.

The elements of the parameter vector Θ for the intervisible networks of the Gulf Test are taken as the coordinates of R flash positions x_i^r, $r = 1, 2, \ldots, R$, and the coordinates of S ground stations, y_i^s, $s = 1, 2, \ldots, S$. (Subscripts always pertain to the 3-vector of cartesian space, and the convention of summation over repeated subscripts is adopted.) Estimates are available before the reduction of the coordinates of the stations $\overset{\circ}{y}{}_i^s \approx y_i^s$ and of their uncertainties. The uncertainties for each station are normally distributed with zero means and inverse covariance elements K_{ij}^s. It is assumed that there is no correlation between stations and that each error ellipsoid defined by K_{ij}^s is an ellipsoid of revolution about the local vertical axis. Properly interpreted, the solution to be derived is valid in the limit as any error ellipsoid becomes infinitesimal (fixed station) or infinite (completely unknown station)

The range from station s to flash r is

$$w^{rs} = \left| x_i^r - y_i^s \right|$$

and the direction cosines from the station to the flash are

$$\mu_i^{rs} = \frac{(x_i^r - y_i^s)}{w^{rs}} .$$

The corresponding observed direction cosines are ν_i^{rs}. It is assumed that the angle ϕ^{rs} between the vectors $\left[\mu_i^{rs}\right]$ and $\left[\nu_i^{rs}\right]$ is normally distributed with zero mean and standard deviation σ^{rs}. For a missing observation, $1/\sigma^{rs}$ is taken as zero. Because ϕ^{rs} is small ($\sim 10^{-5}$),

$$(\phi^{rs})^2 = \sin^2 \phi^{rs} = 1 - \cos^2 \phi^{rs} = 1 - (\mu_i^{rs} \ \nu_i^{rs})^2 .$$

The log likelihood function for this model is

$$L = \text{constant} + \frac{1}{2} \sum_{r=1}^{R} \sum_{s=1}^{S} \left(\frac{\mu_i^{rs} \ \nu_i^{rs}}{\sigma^{rs}} \right)^2 - \frac{1}{2} \sum_{s=1}^{S} (y_i^s - \overset{\circ}{y}{}_i^s) \, K_{ij}^s \, (y_j^s - \overset{\circ}{y}{}_j^s).$$

Its first derivatives are, to the first order in ϕ^{rs},

$$\frac{\partial L}{\partial x_i^r} = \sum_{s=1}^{S} \frac{\nu_i^{rs} - \mu_i^{rs}}{w^{rs} (\sigma^{rs})^2} ,$$

$$\frac{\partial L}{\partial y_i^s} = - \sum_{r=1}^{R} \frac{\nu_i^{rs} - \mu_i^{rs}}{w^{rs} (\sigma^{rs})^2} - K_{ij}^s (y_j^s - \mathring{y}_j^s).$$

Its second derivatives are, to the zeroth order in ϕ^{rs} ($\mu_i^{rs} = \iota_i^{rs}$),

$$\frac{\partial^2 L}{\partial x_i^r \partial y_j^s} = \frac{\delta_{ij} - \mu_i^{rs} \mu_j^{rs}}{(w^{rs} \sigma^{rs})^2},$$

$$\frac{\partial^2 L}{\partial x_i^r \partial x_j^r} = - \sum_{s=1}^{S} \frac{\delta_{ij} - \mu_i^{rs} \mu_j^{rs}}{(w^{rs} \sigma^{rs})^2},$$

$$\frac{\partial^2 L}{\partial y_i^s \partial y_j^s} = - \sum_{r=1}^{R} \frac{\delta_{ij} - \mu_i^{rs} \mu_j^{rs}}{(w^{rs} \sigma^{rs})^2} - K_{ij}^s,$$

where δ_{ij} is the Kronecker delta. All other second derivatives are zero.

The second derivatives are calculated from the first approximations for x_i^r and y_i^s, and the covariance matrix is found by inversion. For reasonable first approximations, this matrix need be evaluated only once. The first derivatives are multiplied by the covariance matrix as in Eq. (1) to generate corrections to x_i^r and y_i^s (that is, to θ^p), which are in turn used to update the first derivatives for iterative application of the equation. Iterations are continued until all the corrections generated are significantly less than the solution variances. The criterion that

$$(\hat{\theta}^p - \tilde{\theta}^p)^2 < 100\, \eta^{pp}, \qquad p = 1, 2, \ldots, P,$$

is usually satisfied by the second iteration of the Gulf Test solution, one application of the first-order solution is therefore usually quite sufficient.

If station s is completely unkown, $K_{ij}^s = 0$ and the above formulas need no modification. If, however, the station is fixed, set $K_{ij}^s = \alpha \delta_{ij}$ and let $\alpha \to \infty$. Then $\frac{\partial^2 L}{\partial y_i^s \partial y_j^s} = -\alpha \delta_{ij}$ and the corresponding elements in the covariance matrix approach $\alpha^{-1} \delta_{ij}$. These elements multiply only $\frac{\partial^2 L}{\partial y_j^s} = -\alpha (y_j^s - \mathring{y}_j^s)$ in the application of Eq. (1), the net result is that any y_i^s are replaced by $\mathring{y}_i^s$ after one iteration, and they are not modified thereafter. In practice this is accomplished simply by dropping y_i^s as adjustment parameters.

The above solution is valid only for intradatum ties, but it can easily be extended for interdatum ties as well. For instance, suppose that for $s = 1, 2, \ldots, T$, $\mathring{y}_i^s$ is referred to one datum, and for $s = T+1, T+2, \ldots, S$, $\mathring{y}_i^s$ is referred to a second datum. Let the datum displacement be z_i, and in all of the above formulas replace $\mathring{y}_i^s$ by $\mathring{y}_i^s + z_i$ when $s > T$. The additional derivatives with respect to z_i of the modified log likelihood function are, to the appropriate order,

$$\frac{\partial L}{\partial z_i} = \sum_{s=T+1}^{S} K_{ij}^s (y_j^s - \mathring{y}_j^s - z_j),$$

$$\frac{\partial^2 L}{\partial z_i \partial z_j} = -\sum_{s=T+1}^{S} K_{ij}^s,$$

$$\frac{\partial^2 L}{\partial z_i \partial y_j^s} = K_{ij}^s, \qquad s > T.$$

All other additional derivatives are zero. With the modified and new derivatives, the datum displacement can be carried along with the coordinates of the stations and flashes in the parameter vector Θ.

An advantage of this type of solution over the usual least squares approach is that if the geometry and precision of a network and its measurements are specified, the covariance matrix can be calculated without requiring actual observations. Thus, error analyses can be performed for hypothetical models. For the Gulf Test measurements, the observed apparent right ascensions and declinations and their standard deviations are calculated in the least squares plate reductions of ACIC. These standard deviations are checked against the solution errors (that is, the magnitudes of the cross products of the solution and observed vectors); in some cases they require modification and second solutions. In such cases, there are slight differences between the solution parameters, but the covariance matrices change moderately.

5. OBSERVATION NETWORK

The eleven PC-1000 camera sites occupied during the Gulf Test are listed in Table 1. Station 650, Jacksonville, and Station 650M, Mulberry, were occupied by the same camera, the camera being at Jacksonville for the first half of the test program. The 1381st Geodetic Survey Squadron of APCS provided the coordinates

TABLE 1. Geodetic coordinates of camera sites, NAD 27

Geographic Site	Station No.	Latitude North (ϕ)	Longitude West (λ)	Height Above Mean Sea Level (h)	Height Above Spheroid (H)
Houma, La.	640	$29^{O}33'44''.80$	$90^{O}40'44''.19$	2.0m	7.0m
Ellington, Tex.	641	$29^{O}35'39''.89$	$95^{O}09'14''.04$	8.2m	12.2m
England, La.	643	$31^{O}19'15''.91$	$92^{O}31'31''.91$	26.8m	29.8m
Corpus Christi, Tex.	644	$27^{O}41'20''.88$	$97^{O}14'36''.88$	3.4m	6.4m
Dauphin I, Ala.	647	$30^{O}14'48''.28$	$88^{O}04'42''.51$	1.2m	5.2m
Hunter, Ga.	648	$32^{O}00'05''.87$	$81^{O}09'13''.64$	12.2m	12.2m
Jupiter, Fla.	649	$26^{O}57'12''.57$	$80^{O}04'55''.80$	6.8m	9.3m
Jacksonville, Fla.	650	$30^{O}14'10''.72$	$81^{O}40'57''.46$	5.8m	9.3m
Mulberry, Fla.	650M	$30^{O}13'05''.46$	$81^{O}41'47''.81$	6.4m	9.9m
Orlando, Fla.	686	$28^{O}34'26''.03$	$81^{O}19'39''.07$	28.6m	33.7m
Orlando, Fla.	686C	$28^{O}34'26''.70$	$81^{O}19'38''.65$	28.6m	33.7m

TABLE 2. Station observations (ANNA satellite altitude approximately 1100 km)

Net No.	Date	Time GMT	Sub-Sat. Lat. N^{O}	Sub-Sat. Lat. W^{O}	Flash Mode	640	641	643	647	648	649	650M
8	1 Oct 63	0955	33	85	Memory		x	x	x	x		
19	22 Oct 63	0347	31	87	EMOS	x		x	x	x		
22	26 Oct 63	0306	26	88	EMOS		x	x	x	x		
28	19 Dec 63	0228	33	90	EMOS	x		x	x	x	x	x
30	20 Dec 63	0149	31	88	EMOS	x			x	x	x	x
34	3 Jan 64	0601	28	92	EMOS	x	x	x	x	x	x	x

of the camera sites, which were tied to first-order control of the North American Datum (NAD 27), ACIC supplied the geoid-spheroid separations necessary to convert heights above mean sea level to heights above the reference spheroid.

Thirty-nine observation nets were obtained in the Gulf Test. (A net is defined as a flash sequence successfully photographed from three or more camera stations.) The analysis in this paper on the capabilities of the PC-1000 camera is based on data currently available (Table 2), obtained from six nets and seven cameras. It is anticipated that all nets will eventually be combined in one overall reduction and published.

6. RESULTS

Four geodetic networks were examined with the intervisible computer program.

In general, the horizontal standard deviations of the stations to be adjusted were chosen as 100 m. Except for one case in which the initial coordinates of one of these stations were deliberately in error by 140 m, these constraints were relatively so weak that they were tantamount to assuming infinite horizontal standard deviations. The horizontal constraint was rather harsh for the station deliberately in error but was offset by the strength of the observations, coupled with the assumption that the locations of the other two stations in that reduction were perfectly known. In general, the vertical standard deviations of the stations to be adjusted were chosen as 5 m. These are reasonable uncertainties for the geoid-spheroid separations in the Gulf Test area. Because of the poor vertical control inherent in the Gulf Test nets, the vertical standard deviations were usually decreased only slightly in the reductions, that is, tight vertical constraints were usually necessary to keep the vertical coordinates from "running away."

The coordinates of Station 640 (Table 3 and Figure 3) were determined from intervisible observations of 10 flashes in Nets 30 and 34, using 648–649 as a baseline. The mean observation standard deviations were 0".85 for Station 648, 1".08 for Station 649, and 1".56 for Station 640.

The coordinates of Stations 648 and 649 were assumed to be perfectly known, but Station 640 was given an input position error of +3" in latitude and -4" in longitude and standard deviations of 100 m in north-south and east-west directions and 5 m in height above the spheroid.

The sizable 640 position error was removed in the reduction, with a resulting distance R of 7.1 m between the NAD 27 position and the ANNA determined position. This corresponds to a proportional accuracy of 1 in 140,000. The square root of the trace of the station solution covariance matrix R_σ is 8.7 m.

A second reduction was done using observation sigmas derived from the first geodetic reduction rather than ACIC plate reduction standard deviations. These

TABLE 3. Geodetic position determination of station 640 from stations 648 and 649

Reference stations 648 and 649	$\sigma_{N\text{-}S} = \sigma_{E\text{-}W} = \sigma_{H} = 0$
Input standard deviations station 640	$\sigma_{N\text{-}S} = 100\text{m}$, $\sigma_{E\text{-}W} = 100\text{m}$, $\sigma_{H} = 5\text{m}$
Input error station 640	$\phi = +3''$, $\lambda = -4''$

Observations: All stations observed 5 flashes each on nets 30 and 34

Average observation σ used: 648, ".85; 649, 1".08; 640, 1".56

	ϕ	λ	H(meters)	R(meters)
North American Datum 27	29° 33' 44".80	90° 40' 44".19	7.0	
ANNA Data Reduction	44".78	43".93	7.6	
Δ	".02	".26	-.6	7.1
σ	".11	".25	4.8	8.7

$R = \left[(\Delta x)^2 + (\Delta y)^2 + (\Delta z)^2\right]^{1/2}$

$R = \left[\sigma_x^2 + \sigma_y^2 + \sigma_z^2\right]^{1/2}$

Distance = 987 km

Proportional Accuracy (NAD Standard)
1/140,000

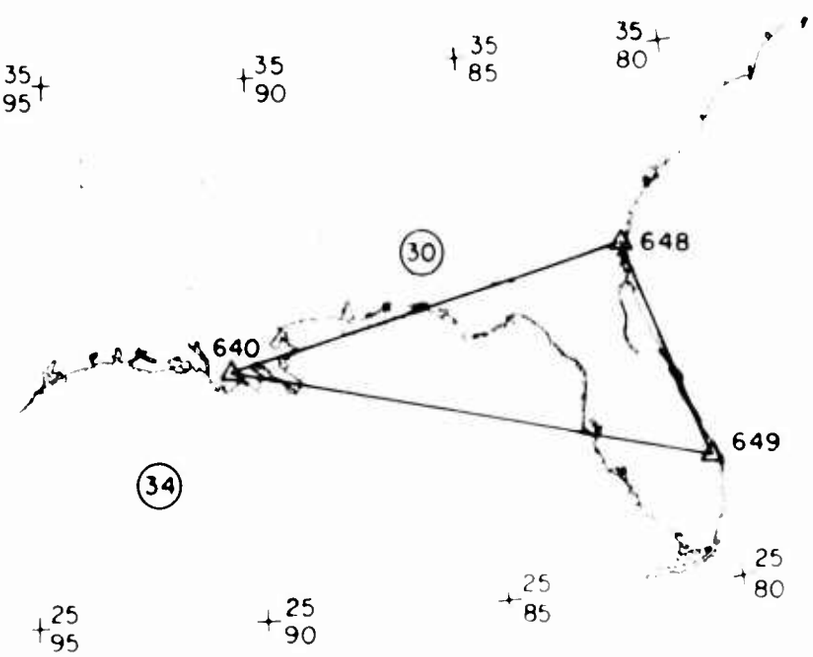

Figure 3. The Coordinates of Station 640 are Determined From Those of Stations 648 and 649 by Nets 30 and 34

sigmas were 1".17 for 648, 1".96 for 649, and 1".69 for 640. With this change in weight, R and R_o become, respectively, 9.8 m and 11.8 m; these results may be more realistic.

In determining the geodetic coordinates of Station 648 (Table 4 and Figure 4), simultaneous observations from 648, 641 and 643 of four flashes in Net 8 and five flashes in Net 22 were used. The average of the observation sigmas were 0".84 for station 641, 0".71 for station 643, and 0".77 for station 648.

Flawless geodetic information was assumed for the known Stations 641 and 643 but the unknown Station 648 was given standard deviations of 100 m in the north-south direction, 100 m in the east-west direction, and 5 m in height.

With a short baseline (317 km) and poor station-satellite geometry, at Station 648 the distance R is 13.4 m. For a distance of 1220 km (the average of Stations 641 to 648 distance and Stations 643 to 648 distance), the proportional accuracy is 1/91,000.

For this reduction, the vertical standard deviation of Station 648 decreased from 5.0 m to 3.8 m. Compared with other runs, this indicates relatively favorable geometry for vertical control. If there had been no vertical constraint, the vertical standard deviation of the solution would have been approximately 6 m.

A comparison of the observational and solution geometries indicated that the flash observation standard deviations were slightly overoptimistic. The computed R_o of 12.0 m is therefore underestimated by perhaps 30%; either way, it is entirely consistent with R.

Of incidental interest are the uncertainties of the final flash positions. The flash error ellipsoids of this reduction are approximately cigar-shaped; the longest axis of each is aligned in the general direction of the 641—643 baseline from the flash location. For flashes in Net 8, the standard deviations along the longest axes and normal to these axes are about 1.5 m and 2.5 m. For flashes in Net 22 these standard deviations are about 12.5 m and 3 m.

Stations 640, 643, and 648 simultaneously observed four flashes of Net 19 and three flashes of Net 28 (Table 5 and Figure 5). Three adjustments were made with the data. The average observation sigmas for each station were as follows: 640, 1".26, 643, 0".83, 638, 0".75. The corresponding sigmas of the second fit were, respectively, 1".03, 1".26, and 0".92.

For the first run the coordinates of the reference Stations 640 and 643 were assumed to be known perfectly. For the second run the reference stations were given horizontal standard deviations of 3 m and vertical standard deviations of 0.1 m, which are still optimistic for NAD 27 first-order stations. For the third run, the horizontal standard deviations were doubled to 6 m and the vertical standard deviations were unchanged. For all runs the unknown Station 648 had horizontal standard deviations of 100 m and a vertical standard deviation of 5.0 m.

TABLE 4. Geodetic position determination of station 648 from stations 641 and 643

Reference stations 641 and 643 $\sigma_{N-S} = \sigma_{E-W} = \sigma_H = 0$

Input standard deviations station 648 $\sigma_{N-S} = 100m$, $\sigma_{E-W} = 100m$, $\sigma_H = 5m$

Observations: All stations observed 4 flashes on net 8 and 5 flashes on net 22

Average observation σ used: 641, ".84; 643, ".71; 648, ".77

	φ	λ	H(meters)	R(meters)
North American Datum 27	32° 00' 05".87	81° 09' 13".64	12.2	
ANNA Data Reduction	06".01	13".18	8.7	
Δ	-".14	".46	3.5	13.4
σ	".11	".43	3.8	12.0

$R = \left[(\Delta x)^2 + (\Delta y)^2 + (\Delta z)^2\right]^{1/2}$

$R_\sigma = \left[\sigma_x^2 + \sigma_y^2 + \sigma_z^2\right]^{1/2}$

Distance: 1220 km

Proportional Accuracy (NAD Standard) 1/91,000

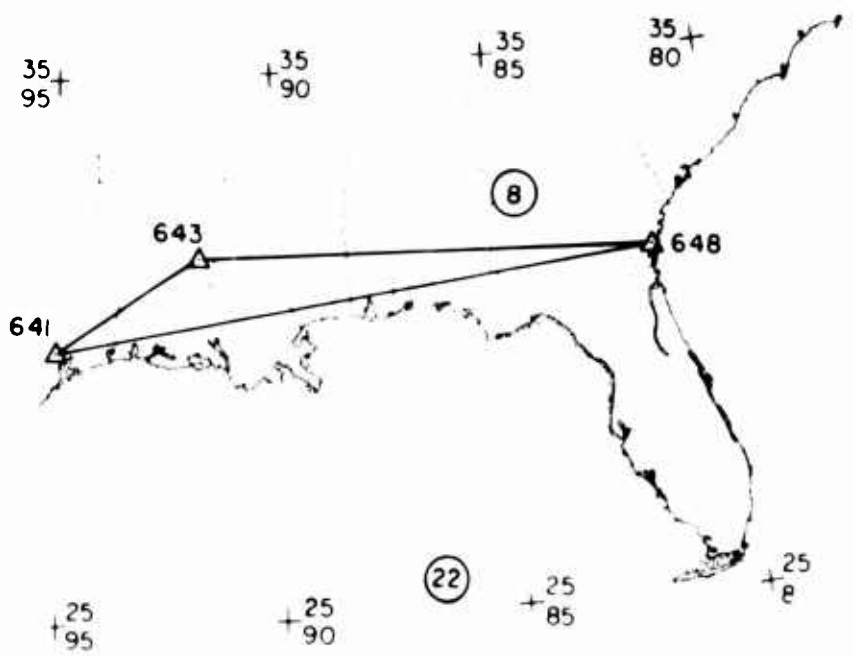

Figure 4. The Coordinates of Station 648 are Determined From Those of Stations 641 and 643 by Nets 8 and 22

TABLE 5. Geodetic position determination of station 648 from stations 640 and 643

Reference stations 640 and 643	Run 1: $\sigma_{N-S} = \sigma_{E-W} = 0m$, $\sigma_H = 0m$ Run 2: $\sigma_{N-S} = \sigma_{E-W} = 3m$, $\sigma_H = 0.1m$ Run 3: $\sigma_{N-S} = \sigma_{E-W} = 6m$, $\sigma_H = 0.1m$
Input standard deviations station 648	$\sigma_{N-S} = 100m$, $\sigma_{E-W} = 100m$, $\sigma_H = 5m$
Observations:	All stations observed 4 flashes on net 19 and 3 flashes on net 28
Average observation σ used:	640, 1".26; 643, ".83, 648, ".75

		ϕ	λ	H(meters)	R(meters)
North American Datum 27		32° 00' 05".87	81° 09' 13".64	12.2	
ANNA Data Reduction	1	05".76	14".47	10.4	
	Δ	+".11	-".83	+1.8	21.7
	σ	".07	".50	4.9	14.6
ANNA Data Reduction	2	05".76	14".44	10.5	
	Δ	+".11	-".80	+1.7	21.3
	σ	".11	".83	4.9	22.2
ANNA Data Reduction	3	05".80	14".26	10.5	
	Δ	+".07	-".62	+1.7	16.5
	σ	".22	1".30	4.9	35.1

$$R = \left[(\Delta x)^2 + (\Delta y)^2 + (\Delta z)^2\right]^{1/2}$$

$$R_\sigma = \left[\sigma_x^2 + \sigma_y^2 + \sigma_z^2\right]^{1/2}$$

Distance 1015 km

Proportional Accuracy (NAD Standard)
Run 1, 1/47,000
Run 2, 1/48,000
Run 3, 1/62,000

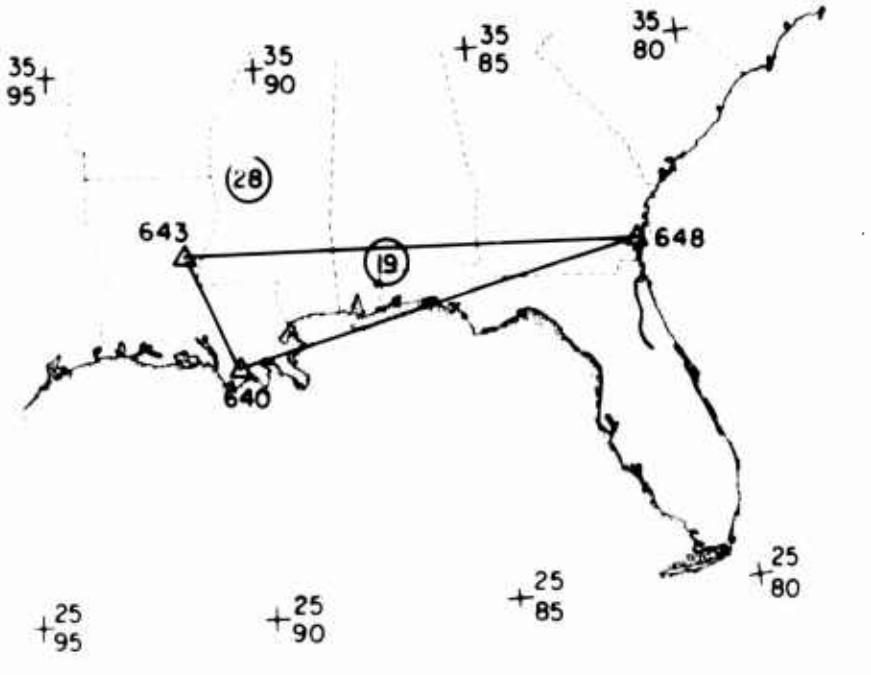

Figure 5. The Coordinates of Station 648 are Determined From Those of Stations 640 and 643 by Nets 19 and 28

The difference between the NAD 27 position and the ANNA determined position for the first run is 21.7 m (R_σ = 14.6 m), which corresponds to 1/47,000. For the second run this difference is 21.3 m (R_σ = 22.2 m) and the proportional accuracy is 1/48,000. For the third run the difference is 16.5 m (R_σ = 35.1 m) and the proportional accuracy is 1/62,000. In each case the major portion of the station error is in the longitude, this is understandable because of the long narrow triangle formed by the stations involved. The reference Stations 640 and 643 have R values of 1 m for the second run and 2 m for the third run; the R_σ of these stations for these runs were not appreciably decreased by the reduction.

It should be noted that geodetic reduction with the above stations using Net 19 (geometrically, much the stronger of the two) alone, produced an R of 3.9 m and an R_σ of 20.6 m. The resultant proportional accuracy of 1/260,000 is deemed fortuitous for so little data.

One overall reduction encompassed four unknown stations (647, 643, 641, and 640), three known stations (648, 649, and 650), and two observation nets (30 and 34). (Table 6 and Figure 6.) As in earlier cases, the known stations were held fixed while the unknown station had standard deviations: σ_{N-S} = 100 m, σ_{E-W} = 100 m, σ_H = 5 m. Ten flashes were observed by all stations except 641 and 643, which observed only the five flashes of Net 34.

Mean observation sigmas were as follows: 0".85 for 648, 1".08 for 649, 1".09 for 650, 1".16 for 647, 1".56 for 640, 0".79 for 643, and 1".19 for 641. Once again a comparison between the solution angular deviations and the observation sigmas indicated the sigmas were slightly overoptimistic and that each R_σ is somewhat underestimated.

The proportional accuracies are 1/122,000 for 640, 1/86,000 for 641, 1/138,000 for 643. In view of the short distance involved (761 km) for the 647 determination, the proportional accuracy of 1/62,000 is not too meaningful.

7. CONCLUSIONS AND RECOMMENDATIONS

The results of the Gulf Test reductions demonstrate that the PC-1000 geodetic stellar camera system is capable of extending geodetic control to a proportional accuracy of better than 1/100,000 when cameras in a network simultaneously observe a flashing satellite beacon.

It is recommended that where the operational requirements exist, PC-1000 camera systems be used to make geodetic ties and strengthen geodetic control by observing the ANNA 1-B satellite. When the ANNA beacon, which is now going into its twenty-first month of operation, ceases to produce the required light output, rocket-borne pyrotechnic flares could serve as intervisible light sources.

Long-range planning should be undertaken so that the maximum operational use can be made of the GEOS satellite beacon when that vehicle is placed in orbit.

TABLE 6. Geodetic position determination of stations 640, 641, 643, and 647 from stations 648, 649, and 650

Reference stations 648, 649, and 650: $\sigma_{N-S} = \sigma_{E-W} = \sigma_H = 0$

Input standard deviations, stations 640, 641, 643, and 647: $\sigma_{N-S} = 100m$, $\sigma_{E-W} = 100m$, $\sigma_H = 5m$

Observations: Stations 648, 649, 650, 640, and 647 observed 5 flashes on Net 30 and 5 flashes on Net 34. Stations 641 and 643 observed 5 flashes on Net 34.

Sta.	Reduction				North American Datum-ANNA Data Reduction						R (meters)	Distance (km)	Proportional Accuracy (NAD Standard)
	σ_ϕ	σ_λ	σ_H	R_σ	$\Delta\phi$	$\Delta\lambda$	ΔH	Δx	Δy	Δz			
640	.11"	.21"	4.7m	8.3m	+".09	+".29	-0.2m	-7.7m	+1.6m	+2.0m	8.1	987	1/122,000
641	.14"	.36"	5.0m	11.7m	-".06	+".61	0.0m	-16.8m	+0.7m	-1.4m	16.9	1454	1/86,000
643	.11"	.29"	5.0m	9.7m	+".09	+".33	-0.4m	-8.3m	+2.5m	+2.5m	9.0	1238	1/138,000
647	.07"	.18"	4.6m	6.9m	+".14	+".42	+0.7m	-11.3m	+1.5m	+4.5m	12.3	761	1/62,000

$$R = \left[(\Delta x)^2 + (\Delta y)^2 + (\Delta z)^2\right]^{1/2}$$

$$R_\sigma = \left[\sigma_x^2 + \sigma_y^2 + \sigma_z^2\right]^{1/2}$$

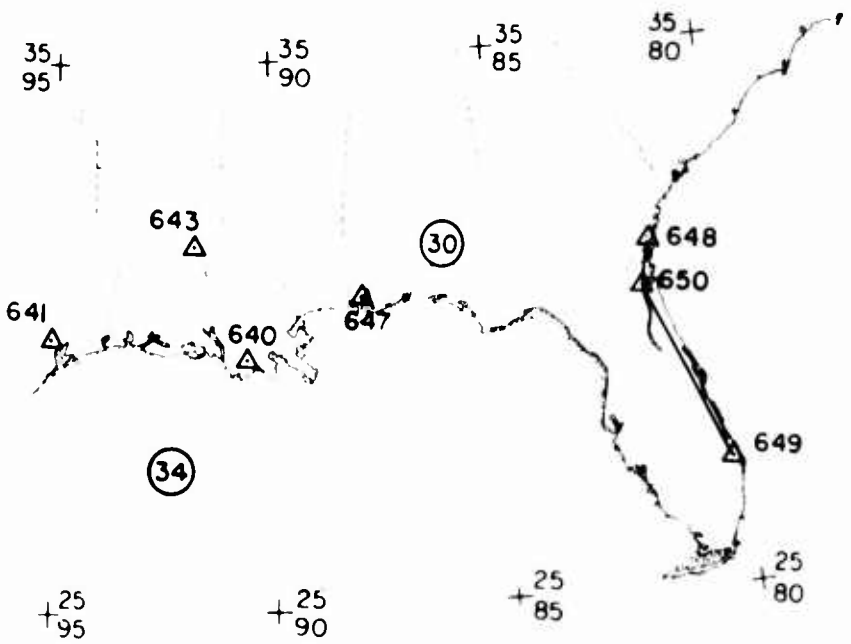

Figure 6. The Coordinates of Stations 640, 641, 643, and 647 are Determined From Those of Stations 648, 649 and 650 by Nets 30 and 34

Acknowledgments

This paper results from the cooperation of APCS camera crews, ACIC plate reduction specialists, and AFCRL geodesists. The excellent computational support by Mr. George Hadgigeorge of AFCRL deserves special mention, as do the efforts of Mr. L. Kuykendall and Mr. J. Bugnitz of ACIC.

References

1. J. P. Rossoni, P. Sconzo, and D. Winfield, Short Arc Orbit Determination for ANNA Satellite, AFCRL-64-273, [Contract AF19(628)-3266], May 1964.

2. A. Mancini, Long Line Azimuths From Optical Observations of the ANNA Flashing Satellite, AFCRL-64-446, [Environmental Research Papers No. 21], May 1964.

3. D. C. Brown, An Advanced Reduction and Calibration for Photogrammetric Cameras, AFCRL-64-40, [Contract AF19(604)-8493], January 1964.

4. R. Moroney, I. Hussey, and W. Nixon, Multi-Angulation Multi-Lateration Programming Report, AFCRL-63-741, [Contract AF19(628)-2379], September 1963.

ENVIRONMENTAL RESEARCH PAPERS

No. 1. Examination of a Wind Profile Proposed by Swinbank, *Morton L. Barad, March 1964 (REPRINT).*

No. 2. Wind and Temperature Variations During Development of a Low-Level Jet, *Yutaka Izumi, Morton L. Barad, March 1964 (REPRINT).*

No. 3. Radiation Pattern of Surface Waves From Point Sources in a Multi-Layered Medium, *N. A. Haskell, March 1964 (REPRINT).*

No. 4. Photoelectric Emission Phenomena in LiF and KCl in the Extreme Ultraviolet, *R. G. Newburgh, February 1964 (REPRINT)*

No. 5. Equatorial Loci of the Earth's Magnetic Field and Cosmic Ray Parameters, *E. J. Chernosky, J. M. Collins, M. P. Hagan, March 1964.*

No. 6. Helium and Argon Emission Continua and Their Use in Absorption Cross-Section Measurements in the Vacuum Ultraviolet, *R. E. Huffman, Y. Tanaka, J. C. Larrabee, March 1964 (REPRINT).*

No. 7. Airflow and Structure of a Tornadic Storm, *K. A. Browning, R. J. Donaldson, Jr., March 1964 (REPRINT).*

No. 8. Automatic Digital Radar Reflectivity Analysis of a Tornadic Storm, *David Atlas, Keith A. Browning, Ralph J. Donaldson, Jr., Hugh J. Sweeney, March 1964 (REPRINT).*

No. 9. Indications of a Lunar Synodical Period in the Sunshine Observations for Boston, Massachusetts, and Columbia, Missouri, *Iver A. Lund, March 1964.*

No. 10. A Search for Rainfall Calendaricities, *Glenn W. Brier, Ralph Shapiro, Norman J. MacDonald, March 1964 (REPRINT).*

No. 11. Lee Wave Clouds Photographed From an Aircraft and a Satellite, *John H. Conover, April 1964 (REPRINT).*

No. 12. Diurnal Variation of the Atmosphere Around 190 Kilometers Derived From Solar Extreme Ultraviolet Absorption Measurements, *L. A. Hall, W. Schweizer, H. E. Hinteregger, April 1964 (REPRINT).*

No. 13. Absorption Coefficients of Oxygen in the 1060-580-A Wavelength Region, *R.E. Huffman, J.C. Larrabee, and Y. Tanaka, May 1964 (REPRINT).*

No. 14. Sunrise Effects on East-West Ionospheric Propagation Paths, *Thomas D. Conley and David Blood, May 1964.*

No. 15. Project Firefly 1962-1963, *N.W. Rosenberg, Ed., May 1964.*

No. 16. Small-Scale Wind Structure Above 100 Kilometers, *Samuel P. Zimmerman, May 1964, (REPRINT).*

No. 17. Resonance Radiation of AlO From Trimethyl Aluminum Released Into the Upper Atmosphere, *N.W. Rosenberg, D. Golomb, E.F. Allen, Jr., May 1964, (REPRINT).*

No. 18. Possibility of a 26- or 27-Month Periodicity in the Equatorial Geomagnetic Field, *Ralph Shapiro and Fred Ward, May 1964, (REPRINT).*

No. 19. Crater Frequency and the Interpretation of Lunar History, *Robert T. Dodd, Jr., John W. Salisbury, and Vern C. Smalley, May 1964, (REPRINT).*

No. 20. Altitude Variation of Rayleigh, Aerosol, and Ozone Attenuating Components in the Ultraviolet Region, *L. Elterman, May 1964.*

No. 21. Long Line Azimuths From Optical Observations of the ANNA Flashing Satellite, *Armando Mancini, June 1964.*

No. 22. Ionospheric Perturbations, Solar Flares, and Geomagnetic Storms—Correlations Observed by Oblique Long-Range High-Frequency Probing, *Helen R. Baker and Alfred E. Reilly, June 1964.*

No. 23. Laser-Satellite Reflection Parameters, *Robert L. Iliff, June 1964.*

No. 24. The Infrared Telluric Absorption Spectrum Introductory Report, *J.N. Howard, and J.S. Garing, June 1964 (REPRINT).*

No. 25. Be^7, P^{32} P^{33}, and S^{35}: Stratospheric Concentrations and Artificial Production, *P.J. Dreyinsky, J.T. Wasson, E.C. Couble and V.A. Dimond, July 1964 (REPRINT).*

No. 26. Generation and Properties of High Altitude Chemical Plasma Clouds, *N.W. Rosenberg and D. Golomb, July 1964 (REPRINT).*

No. 27. The Statistics of Satellite Scintillations at a Subauroral Latitude, *Jules Aarons, John Mullen and Sunanda Basu, July 1964 (REPRINT).*

No. 28. The Mathematical Equivalence of Multi-Level and Vertically Integrated Numerical Forecasting Models, *Louis Berkofsky, July 1964 (REPRINT).*

No. 29. Low Energy Charge Exchange and Ion-Molecule Reactions, *J.F. Paulson, July 1964 (REPRINT)*

ENVIRONMENTAL RESEARCH PAPERS (Continued)

No. 30. Shear Deformation of Upper Mantle Mineral Analogues: Tests to 55 kb at 25°C, *R.E. Riecker, 1 Lt, USAF, and K.E. Seifert, 1 Lt, USAF, July 1964.*

No. 31. Some Numerical Results of a Model Investigation of the Atmospheric Response to Upper-Level Heating, *Louis Berkofsky and Ralph Shapiro, July 1964 (REPRINT).*

No. 32. Electrical Processes in the Nighttime Exosphere, *K.C. Sagalyn and M. Smiddy, July 1964 (REPRINT).*

No. 33. Radioactivity in Sputnik 4 Fragment, *John T. Wasson, July 1964 (REPRINT).*

No. 34. Falling Sphere Measurements of Atmospheric Density, Temperature, and Pressure, up to 115 km, *A.C. Faire and K.S.W. Champion, July 1964.*

No. 35. Geodetic Positioning From Simultaneous Optical Observations of the ANNA 1-B Satellite, *Lyndon L. Sheldon, Capt, USAF, and Donald H. Eckhardt, July 1964.*